2.5D MULTIZONE REPRODUCTION USING WEIGHTED MODE MATCHING

Wen Zhang[1,2]*, Junqing Zhang*[1]*, Thushara D. Abhayapala*[2]*, and Lijun Zhang*[1]

[1]Center of Intelligent Acoustics and Immersive Communications
Northwestern Polytechnical University, Xi'an, Shaanxi 710072, China
[2]Research School of Engineering, College of Engineering and Computer Science
The Australian National University, Canberra, ACT 0200, Australia

ABSTRACT

The mode matching based multizone reproduction has mainly been focused on a purely 2D theory which is inadequate to fit the 3D reality. Its extension to the 3D theory however requires many secondary sources and a high computational complexity. In this paper, a weighted mode matching approach is developed for 2.5D multizone reproduction. The multizone soundfield is reproduced in the horizontal plane within a circular control region using the loudspeakers modelled as 3D point sources. We propose weighting the Bessel-spherical harmonic modes for 2.5D reproduction and a matching between the desired and reproduced soundfields over the entire control region. Simulation results show that in comparison with the conventional 2.5D reproduction method a more accurate reproduction is achieved using the proposed weighting approach.

Index Terms— Multizone reproduction, 2.5D reproduction, mode matching, weighting approach, reverberant rooms

1. INTRODUCTION

Multizone reproduction aims to reproduce sounds over multiple regions of space simultaneously and independently using a single array of loudspeakers [1]. This arrangement allows sound zones to be produced at any desired location and also the listener to freely move between zones thus can provide significant flexibility and has a wide range of audio applications [2, 3]. Some well-known methods for multizone reproduction include acoustic contrast control (ACC) [4-8], pressure matching (PM) [9-12], the combination of ACC and PM [13-16], and mode matching based reproduction [17-20].

While the ACC and PM methods focus on point-to-point audio processing, the mode matching approach is based on representing the soundfields within different zones through a spatial harmonic expansion. The local soundfield coefficients are transformed to an equivalent global soundfield using the harmonic translation theorem and the loudspeaker weights are designed to create this global desired soundfield [17-21]. The mode matching approach can provide insights into the multizone problem. For example, through the modal domain analysis, a theoretical basis is established for creating two sound zones with no interference [19]. Modal-domain sparsity analysis shows that a significantly reduced number of microphone points could be used quite effectively for multizone reproduction over a wide frequency range [18]. A parameter, the coefficient of realisability, is developed to quantitatively analyze the achievable reproduction performance [20].

e-mail: wen.zhang@nwpu.edu.cn

This work was supported by the National Natural Science Foundation of China (NSFC) funding scheme under Project No. 61671380.

The mode matching approach however has been mainly considered in the two-dimensional (2D) case, i.e., both the virtual source generating the desired soundfield and the secondary source used for reproduction are modelled as 2D near-field or far-field sources. Even though the theory can be easily extended to the three-dimensional (3D) case. Given the same reproduction setup, the 3D approach that controls sound within a sphere requires many secondary sources and a higher computational complexity.

In this work, we investigate the problem of controlling 2D multizone soundfields using 3D secondary sources. This is a more practical setup as on the one hand the same number of loudspeakers as in the 2D reproduction is required and on the other hand loudspeakers are more accurately modelled as 3D point sources. However, there is intrinsic dimensionality mismatch between the 2D desired soundfields and 3D secondary sources, also known as *2.5D reproduction* [22-26]. To solve the dimensionality mismatch problem, the mode matching approach is applied where the desired and generated soundfields are decomposed through spatial harmonics and the matching at the center of the setup is applied. Analytical solutions are derived for a circular array of secondary sources [23-25,27]. However, this approach has mainly been verified for the single zone case, which is also located at the center.

We propose a weighted mode matching approach for 2.5D multizone reproduction in this paper based on the concept outlined in [18] for 2D and 3D reproduction. Instead of referencing the synthesized soundfield to the desired one at a particular point or radius, the matching is over the entire control region. This is based on weighting the Bessel-spherical harmonic modes. The 2D multizone reproduction using mode matching is revisited in Sec. 2. Section 3 introduces the dimensionality mismatching problem in 2.5D reproduction and proposed two weighted mode matching algorithms. In Sec. 4, the proposed methods are evaluated in comparison with the conventional 2.5D reproduction approach.

2. REVIEW: 2D MULTIZONE REPRODUCTION

The objective of the general multizone problem is to produce a desired spatial soundfield in each of Q non-overlapping sound zones. As shown in Fig. 1, we assume that each sound zone q has a radius R_q and its centre is denoted by $\boldsymbol{O}_q$ with respect to the global origin $\boldsymbol{O}$. Any observation point within a sound zone is represented by $\boldsymbol{x}_q$ with respect to $\boldsymbol{O}_q$, or $\boldsymbol{x} = \boldsymbol{x}_q + \boldsymbol{O}_q$ with respect to $\boldsymbol{O}$. All sound zones are within a general region of interest of radius $r \leq r_0$.

2.1. Soundfield model

The soundfield at any point $\boldsymbol{x}_q \equiv (\|\boldsymbol{x}_q\|, \hat{\boldsymbol{x}}_q)$ within a sound zone in 2D cylindrical coordinates can be expressed in the form

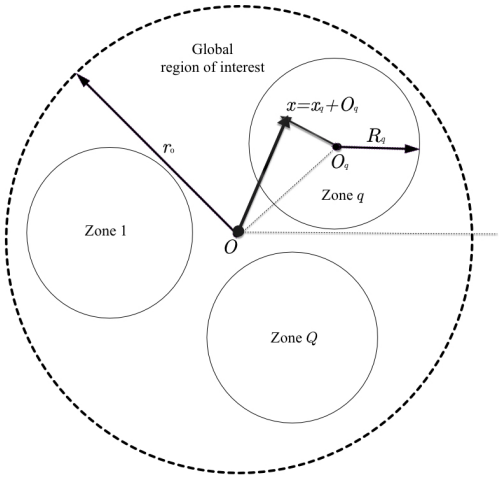

Fig. 1. Geometry of multizone reproduction.

$$P_d^{(q)}(\boldsymbol{x}_q,k) \approx \sum_{m'=-N_q}^{N_q} \alpha_{m'}^{(q)}(k) J_{m'}(k\|\boldsymbol{x}_q\|) e^{im'\hat{\boldsymbol{x}}_q} \tag{1}$$

where $\hat{\boldsymbol{x}}_q = \phi_{\boldsymbol{x}_q}$, $k = 2\pi f/c$ is the wave number with f being the frequency and c the speed of sound. $J_{m'}(k\|\boldsymbol{x}_q\|)$ is the cylindrical Bessel function of order m', and $\alpha_{m'}^{(q)}(k)$ is the corresponding m'th order soundfield coefficient to describe a spatial soundfield with respect to $\boldsymbol{O}_q$. Given the radius of the local sound zone R_q, the wave number k, the truncation order is $N_q = \lceil ekR_q/2 \rceil$ [27], where $\lceil\cdot\rceil$ denotes the ceiling function and e is the Euler's number.

Analogous to (1), the soundfield at the point $\boldsymbol{x} = (\|\boldsymbol{x}\|, \hat{\boldsymbol{x}})$ in the global system can be represented by a finite number of cylindrical harmonics

$$P_d(\boldsymbol{x},k) \approx \sum_{m=-N_0}^{N_0} \beta_m(k) J_m(k\|\boldsymbol{x}\|) e^{im\hat{\boldsymbol{x}}}, \tag{2}$$

where $N_0 = \lceil ekr_0/2 \rceil$ and r_0 is the radius of the general region of interest including all sound zones.

These local soundfield coefficients $\alpha_{m'}^{(q)}(k)$ can be related to the global soundfield coefficients $\beta_m(k)$ using the Bessel function addition theorem [28], that is

$$J_m(k\|\boldsymbol{x}\|)e^{im\hat{\boldsymbol{x}}} = \sum_{m'=-N_q}^{N_q} J_{m-m'}(kr_q) e^{i(m-m')\phi_q} J_{m'}(k\|\boldsymbol{x}_q\|) e^{im'\hat{\boldsymbol{x}}_q} \tag{3}$$

given $\boldsymbol{x} = \boldsymbol{x}_q + \boldsymbol{O}_q$ and $\boldsymbol{O}_q \equiv \{r_q, \phi_q\}$ in the global system.

Using the matrix-vector notation, we have

$$\boldsymbol{a}_q = \boldsymbol{T}_q \boldsymbol{b}, \tag{4}$$

where $\boldsymbol{a}_q = [\alpha_{-N_q}^{(q)}(k), \ldots, \alpha_{N_q}^{(q)}(k)]^T$ and $\boldsymbol{b} = [\beta_{-N_0}(k), \ldots, \beta_{N_0}(k)]^T$ are column vectors of length $(2N_q+1)$ and $(2N_0+1)$, respectively. $\boldsymbol{T}_q$ is the $(2N_q+1)\times(2N_0+1)$ matrix representing the translation from the global system to the local system, that is $[\boldsymbol{T}_q]_{m'+N_q+1,m+N_0+1} = J_{m-m'}(kr_q)e^{i(m-m')\phi_q}$.

2.2. Lagrangian formulation and control

The multizone reproduction problem in the modal domain is formulated as finding the global soundfield coefficients $\boldsymbol{b}$ to generate a desired soundfield in the bright zone $\mathbb{D}_\mathrm{b}$ characterised by its local coefficients $\boldsymbol{a}_\mathrm{b}$ with constraints on the sound energy in the dark zone $\mathbb{D}_\mathrm{d}$ and the energy of the entire global soundfield [20]. That is

$$\min_{\boldsymbol{b}} \quad \|\boldsymbol{T}_\mathrm{b}\boldsymbol{b} - \boldsymbol{a}_\mathrm{b}\|^2 \tag{5}$$

$$\text{subject to} \quad \|\boldsymbol{T}_\mathrm{d}\boldsymbol{b}\|^2 \le e_\mathrm{d} \tag{5a}$$

$$\|\boldsymbol{b}\|^2 \le e_\mathrm{g}. \tag{5b}$$

$\boldsymbol{T}_\mathrm{b}$ and $\boldsymbol{T}_\mathrm{d}$ are the translation matrices of the local bright zone and dark zone from the global system, respectively.

We write the optimisation problem posed in Eq. (5) as a Lagrange cost function,

$$\underset{\boldsymbol{b}}{\operatorname{argmin}}\ L(\boldsymbol{b}) = \|\boldsymbol{T}_\mathrm{b}\boldsymbol{b} - \boldsymbol{A}_\mathrm{b}\|^2 + \lambda_1(\|\boldsymbol{T}_\mathrm{d}\boldsymbol{b}\|^2 - e_\mathrm{d}) + \lambda_2(\|\boldsymbol{b}\|^2 - e_\mathrm{g}), \tag{6}$$

where λ_1 and λ_2 are positive Lagrange multipliers. The solution that minimises $L(\boldsymbol{b})$ is

$$\boldsymbol{b} = [\boldsymbol{T}_\mathrm{b}^*\boldsymbol{T}_\mathrm{b} + \lambda_1\boldsymbol{T}_\mathrm{d}^*\boldsymbol{T}_\mathrm{d} + \lambda_2\boldsymbol{I}]^{-1}\boldsymbol{T}_\mathrm{b}^*\boldsymbol{a}_\mathrm{b}, \tag{7}$$

where $(\cdot)^*$ denotes the Hermitian transpose and $\boldsymbol{I}$ is an identity matrix of dimension $2N_0+1$. This formulation can easily be extended to the case of Q sound zones, by augmenting additional dark zone constraints of the form of (5a) to the Lagrange cost function (6).

3. PROPOSED 2.5D REPRODUCTION

3.1. Theory

An array of L loudspeakers is used for reproduction and its generated global soundfield can be written as

$$P(\boldsymbol{x},k) = \sum_{\ell=1}^{L} d_\ell(k) G_\ell(\boldsymbol{x},k), \tag{8}$$

where $G_\ell(\boldsymbol{x},k)$ represents the acoustic transfer function (ATF) between the ℓth loudspeaker and the observation point $\boldsymbol{x}$ in the global system and d_ℓ is the loudspeaker weight.

The ATF is parameterised in the modal domain as

$$G_\ell(\boldsymbol{x},k) \approx \sum_{m=-N_0}^{N_0} \sum_{n=|m|}^{N_0} \gamma_n^m(\ell,k) j_n(k\|\boldsymbol{x}\|) Y_n^m(\frac{\pi}{2}, \phi_{\boldsymbol{x}}) \tag{9}$$

where $\gamma_n^m(\ell,k)$ is an ATF coefficient for source ℓ. Note that each loudspeaker is a 3D point source, there are $(N_0+1)^2$ coefficients to describe its ATF within the global control region. The ATF coefficients are assumed to be a prior knowledge obtained from theoretical solutions or pre-calibration [29]. In anechoic condition, $\gamma_n^m(\ell,k) = -ikh_n^{(2)}(kr_\ell)\overline{Y_n^m(\pi/2,\phi_\ell)}$, where $\overline{(\cdot)}$ represents the complex conjugate.

Then, the generated 3D soundfield is

$$P(\boldsymbol{x},k) \approx \sum_{m=-N_0}^{N_0} \sum_{\ell=1}^{L} d_\ell(k) \underbrace{\sum_{n=|m|}^{N_0} \gamma_n^m(\ell,k) j_n(k\|\boldsymbol{x}\|) Y_n^m}_{h_m(l,k,\|\boldsymbol{x}\|)} e^{im\phi_{\boldsymbol{x}}}, \tag{10}$$

where the spherical harmonic function is written $Y_n^m(\pi/2,\phi)= Y_n^m e^{im\phi}$ with $Y_n^m \triangleq C_n^m P_n^m(0)$ and $C_n^m = \sqrt{\frac{2n+1}{4\pi}\frac{(n-|m|)!}{(n+|m|)!}}$.

Referring to (2), the global desired soundfield is written

$$P_d(\boldsymbol{x},k) \approx \sum_{m=-N_0}^{N_0} \underbrace{\beta_m(k) J_m(k\|\boldsymbol{x}\|)}_{b_m(k,\|\boldsymbol{x}\|)} e^{im\phi_{\boldsymbol{x}}}. \tag{11}$$

Due to the dimensionality mismatch between the 2D desired soundfield and 3D secondary sources, the problem of 2.5D reproduction is to match the $2N_0+1$ azimuthal terms

$$\sum_{\ell=1}^{L} d_\ell(k) h_m(\ell,k,r) = b_m(k,r), \tag{12}$$

at some reference distance r with $r \le r_0$. In the existing methods, the matching point is simply the center of the setup, i.e., the global origin at $r=0$ [23-27]. However, for multizone reproduction, local sound zones are normally away from the center. We propose a matching over the entire global region, i.e., the reference distance $r \in [0, r_0]$, as shown in the following.

3.2. Algorithm 1: Weighted mode matching

Here, we propose the cost function

$$\mathcal{J}(\boldsymbol{d},k) = \frac{1}{2\pi}\int_{\mathbb{D}} \Big| P(\boldsymbol{x}) - P_d(\boldsymbol{x}) \Big|^2 d\boldsymbol{x}. \tag{13}$$

Substituting (10) and (11) into (13) leads to

$$\mathcal{J}(\boldsymbol{d},k) = \sum_{m=-N_0}^{N_0} \int_0^{r_0} \Big| \sum_{\ell=1}^{L} d_\ell(k) h_m(\ell,r,k) - b_m(r,k) \Big|^2 r dr. \tag{14}$$

Writing (14) in the matrix form, we have

$$\mathcal{J}(d,k) = \boldsymbol{d}^H \boldsymbol{\mathcal{H}} \boldsymbol{d} - \boldsymbol{\mathcal{B}}^H \boldsymbol{d} - \boldsymbol{d}^H \boldsymbol{\mathcal{B}} + C. \tag{15}$$

where,

$$[\boldsymbol{\mathcal{H}}]_{\ell_1,\ell_2} = \sum_{m=-N_0}^{N_0} \sum_{n=|m|}^{N_0} \sum_{n'=|m|}^{N_0} \omega_{n,n'}^m \overline{\gamma_n^m(\ell_1,k)} \gamma_{n'}^m(\ell_2,k)$$

$$[\boldsymbol{\mathcal{B}}]_{\ell_1} = \sum_{m=-N_0}^{N_0} \sum_{n=|m|}^{N_0} \chi_n^m \overline{\gamma_n^m(\ell_1,k)} \beta_m(k)$$

and

$$\omega_{n,n'}^m \triangleq Y_n^m Y_{n'}^m \int_0^{r_0} j_n(kr) j_{n'}(kr) r dr$$

$$\chi_n^m \triangleq Y_n^m \int_0^{r_0} j_n(kr) J_m(kr) r dr$$

We write

$$\boldsymbol{\mathcal{H}} = \boldsymbol{\Gamma}^H \boldsymbol{W} \boldsymbol{\Gamma}, \tag{16}$$

where $\boldsymbol{\Gamma}$ is the ATF coefficient matrix defined as $[\boldsymbol{\Gamma}]_{n^2+n+m+1,\ell} = \gamma_n^m(\ell,k)$ and $\boldsymbol{W}$ is a $(N+1)^2$-square weighting matrix defined as

$$[\boldsymbol{W}]_{n^2+n+m+1,n'^2+n'+m'+1} = \delta_{m-m'} w_{n,n'}^m.$$

Similarly, it can be defined that $\mathcal{B} = \boldsymbol{\Gamma}^H \boldsymbol{X} \boldsymbol{b}$, where

$$[\boldsymbol{X}]_{n^2+n+m+1,m'+N_0+1} = \delta_{m-m'} \chi_n^m$$

and $[\boldsymbol{b}]_{m+N_0+1} = \beta_m$.

Minimizing $\mathcal{J}$ in (15), the solution is

$$\widehat{\boldsymbol{d}} = \boldsymbol{\mathcal{H}}^{-1} \boldsymbol{\mathcal{B}} = (\boldsymbol{\Gamma}^H \boldsymbol{W} \boldsymbol{\Gamma})^{-1} \boldsymbol{\Gamma}^H \boldsymbol{X} \boldsymbol{b}. \tag{17}$$

3.3. Algorithm 2: Sectorial weighted mode matching

Sectorial mode matching is the most widely used 2.5D reproduction method, where only the sectorial modes at $n=|m|$ are matched and the matching point is at the global origin $r=0$ [23-27].

Here, we remove the requirement of the matching at the center and apply the weighting approach to the sectorial mode matching. That is, for the sectorial mode approximation,

$$h_m^{\text{sect}}(\ell,k,r) = \gamma_{|m|}^m(\ell,k) j_{|m|}(kr) Y_{|m|}^m. \tag{18}$$

Then, we have

$$\boldsymbol{\mathcal{H}}_{\text{sect}} = \boldsymbol{\Gamma}_{\text{sect}}^H \boldsymbol{W}_{\text{sect}} \boldsymbol{\Gamma}_{\text{sect}}, \tag{19}$$

where $\boldsymbol{\Gamma}_{\text{sect}}$ is a matrix of size $(2N_0+1)\times L$, i.e., $[\boldsymbol{\Gamma}_{\text{sect}}]_{m+N_0+1,\ell} = \gamma_{|m|}^m(\ell,k)$, and the diagonal weighting matrix

$$[\boldsymbol{W}_{\text{sect}}]_{m+N_0+1,m+N_0+1} = [Y_{|m|}^m]^2 \int_0^{r_0} [j_{|m|}(kr)]^2 r dr$$

is of size $(2N_0+1)\times(2N_0+1)$.

Given the global soundfield coefficients $\boldsymbol{b}$ and

$$[\boldsymbol{X}_{\text{sect}}]_{m+N_0+1,m+N_0+1} = Y_{|m|}^m \int_0^{r_0} j_{|m|}(kr) J_m(kr) r dr,$$

the solution for the sectorial weighted mode matching is

$$\widehat{\boldsymbol{d}}_{\text{sect}} = \boldsymbol{\mathcal{H}}_{\text{sect}}^{-1} \boldsymbol{\mathcal{B}}_{\text{sect}} = (\boldsymbol{\Gamma}_{\text{sect}}^H \boldsymbol{W}_{\text{sect}} \boldsymbol{\Gamma}_{\text{sect}})^{-1} \boldsymbol{\Gamma}_{\text{sect}}^H \boldsymbol{X}_{\text{sect}} \boldsymbol{b}. \tag{20}$$

Comments:

- In (17) and (20), the matrices $\boldsymbol{\mathcal{H}}$ and $\boldsymbol{\mathcal{H}}_{\text{sect}}$ are square matrices of size $L \times L$. It shows that the proposed solutions minimize the mean squared error without approximation and no regularization is required.
- The weighting functions, $\boldsymbol{W}$ and $\boldsymbol{X}$, in (17) involve computing the integrals of Bessel-spherical harmonic modes in r at each frequency. The sectorial weighted mode matching has reduced computational complexity but only slightly improved performance as shown in Sec. 4.2.

4. EVALUATION

In this section, the setup and performance of the proposed 2.5D multizone reproduction are described.

4.1. Simulation setup

We simulate two-zone reproduction examples in a reverberant room of size 5×7 m. Room reverberation is simulated using the image source method with the image order up to 5 [30]. The wall reflection coefficient is 0.7 and a perfectly-absorbing surface is assumed for the floor and ceiling. The virtual source, which is located in the far field and incident from $\phi_V = \pi/3$, produces a monochromatic 2D plane wave of frequency 500 Hz. Reproduction on the 2D plane is within a circular control region of radius $r_0 = 2$ m. In the two-zone example, the bright zone and dark zone are located at $\boldsymbol{O}_{\text{b}} = (1.4, 0)$ and $\boldsymbol{O}_{\text{d}} = (-1.4, 0)$ with respect to the global origin, respectively. Each sound zone has a radius of 0.4 m. A uniform circular array of 35 loudspeakers 3 m away from the centre of the global region is used for reproduction, where each loudspeaker is modelled as a 3D point source. The Lagrange multipliers to solve the global soundfield coefficients from (7) are set as $\lambda_1 = 0.2$ and $\lambda_2 = 10^{-3}$.

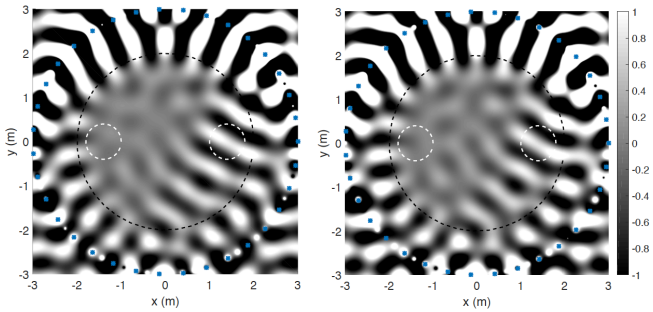

Fig. 2. Reconstructed soundfields using the proposed (a) WMM and (b) SWMM methods. The area within the black dashed line and white dashed line correspond to the global region, local bright zone and dark zone, respectively. Blue $*$ marks denote the locations of 35 loudspeakers.

The performance measures are the acoustic contrast κ between the bright zone and dark zone, and the bright zone reproduction error ε, i.e.,

$$\kappa(k) = 10\log_{10}\frac{\frac{1}{\mathbb{V}_\mathrm{b}}\int_{\mathbb{D}_\mathrm{b}}|P(\boldsymbol{x},k)|^2 d\boldsymbol{x}}{\frac{1}{\mathbb{V}_\mathrm{d}}\int_{\mathbb{D}_\mathrm{d}}|P(\boldsymbol{x},k)|^2 d\boldsymbol{x}} \tag{21}$$

$$\varepsilon(k) = 10\log_{10}\frac{\int_{\mathbb{D}_\mathrm{b}}|P(\boldsymbol{x},k)-P_d(\boldsymbol{x},k)|^2 d\boldsymbol{x}}{\int_{\mathbb{D}_\mathrm{b}}|P_d(\boldsymbol{x},k)|^2 d\boldsymbol{x}}, \tag{22}$$

where $P(\boldsymbol{x},k)$ and $P_d(\boldsymbol{x},k)$ represent the reproduced soundfield and the desired soundfield at a point within the bright zone $\mathbb{D}_\mathrm{b}$ or the dark zone $\mathbb{D}_d$. $\mathbb{V}_b$ and $\mathbb{V}_d$ denote the area of the bright zone and the dark zone, respectively.

4.2. Simulation results

The proposed weighted mode matching (WMM) and sectorial weighted mode matching (SWMM) methods are evaluated in comparison with the conventional sectorial mode matching (SMM) used in 2.5D reproduction. The real part of the reproduced soundfields using the SMM and SWMM approaches are plotted in Fig. 2. The display is limited to the maximum value of the reconstructed field within the bright zone, i.e., acoustic pressure greater than 1 are white and less than -1 are black. Above 15 dB acoustic contrast and less than -10 dB bright zone reproduction error are achieved using the proposed methods.

In the previous example, the distance between the bright zone or dark zone center and the global origin is 1.4 m. Next, we evaluate the system performance under different values of the distance between the zone center and the global origin. The results are shown in Fig. 3. The conventional SMM has the lowest bright zone reproduction error when the distance is less than 0.5 m as shown in Fig. 3 (b). This corresponds to the case that the sound zones are close to the global origin, i.e., the matching point at the center of the setup. On the other hand, the proposed WMM has the highest acoustic contrast over the entire distance range and also the best bright zone reproduction performance when the distance is above 0.5 m. Compared with SMM, the proposed SWMM only shows marginal improvement of bright zone reproduction accuracy when the sound zones are further away from the center.

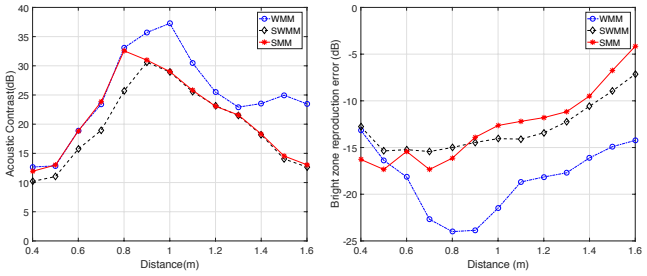

Fig. 3. Plots show (a) acoustic contrast and (b) bright zone error at different distances between the bright zone or dark zone center and the global origin using WMM, SWMM and SMM.

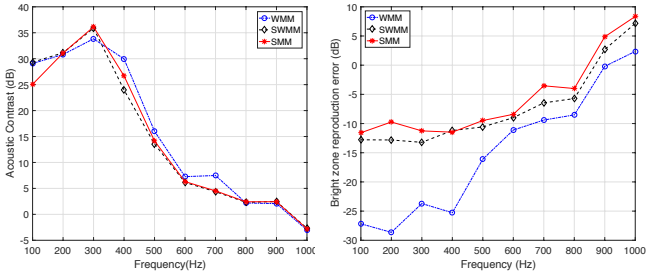

Fig. 4. Plots show (a) acoustic contrast and (b) bright zone error over a broadband frequency range using WMM, SWMM and SMM.

Finally, we compare these three methods over a broadband frequency range of $[0.1, 1]$ kHz. The reproduction setup is the same as in the example of Fig. 2. Notice that in this case, the system, i.e., the number of modes and loudspeakers for soundfield representation and reproduction, is designed at the frequency of 500 Hz [1]. The general trend is that the system designed at a particular frequency can produce satisfied results for frequencies less than the designed value. However, its performance degrades significantly when the frequency is above the design frequency. These three methods have roughly the same acoustic contrast performance while WMM applies the weighting over the region of interest thus has the lowest bright zone reproduction error. SWMM performs slightly better than SMM in terms of bright zone reproduction accuracy.

5. CONCLUSION

The weighted mode matching approach has been proposed in this work for the 2.5D multizone soundfield reproduction problem. The method is based on weighting the Bessel-spherical harmonic modes over the entire global control region. Through simulations, we show that the proposed methods better match the bright zone soundfield than the previous approach such as sectorial mode matching especially when the sound zone is away from the global center. The proposed weighted mode matching method demonstrates the best reproduction performance in a reverberant room and over a wide frequency range.

[1] The approach is applicable to speech or music reproduction but the number of speakers increases with the frequency and global region radius.

6. REFERENCES

[1] T. Betlehem, W. Zhang, M. A. Poletti, and T. D. Abhayapala, "Personal sound zones: Delivering interface-free audio to multiple listeners," *IEEE Signal Processing Magazine*, vol. 32, no. 2, pp. 81–91, 2015.

[2] J. Cheer, S. J. Elliott, and M. F. S. Gálvez, "Design and implementation of a car cabin personal audio system," *J. Audio Eng. Soc.*, vol. 61, no. 6, pp. 414–424, 2013.

[3] T. D. Abhayapala and Y. Wu, "Spatial soundfield reproduction with zones of quiet," in *Proc. 127th Audio Engineering Society Convention*, New York, NY, Oct. 2009, pp. 1-7.

[4] J-W. Choi and Y-H. Kim, "Generation of an acoustically bright zone with an illuminated region using multiple sources," *J. Acoust. Soc. Am.*, vol. 111, no. 4, pp. 1695–1700, 2002.

[5] M. Shin, S. Q. Lee, F. M. Fazi, P. A. Nelson, D. Kim, S. Wang, K. H. Park, and J. Seo, "Maximization of acoustic energy difference between two spaces," *J. Acoust. Soc. Am.*, vol. 128, no. 1, pp. 121–131, 2010.

[6] S. J. Elliott, J. Cheer, J-W. Choi, and Y-H. Kim, "Robustness and regularization of personal audio systems," *IEEE Trans. Audio, Speech, and Language Process.*, vol. 20, no. 7, pp. 2123–2133, 2012.

[7] P. Coleman, P. J. Jackson, M. Olik, and J. A. Pederson, "Personal audio with a planar bright zone," *J. Acoust. Soc. Am.*, vol. 136, no. 4, pp. 1725–1735, 2014.

[8] P. Coleman, P. J. Jackson, M. Olik, M. Møller, M. Olsen, and J. A. Pederson, "Acoustic contrast, planarity and robustness of sound zone methods using a circular loudspeaker array," *J. Acoust. Soc. Am.*, vol. 135, no. 4, pp. 1929–1940, 2014.

[9] M. A. Poletti, "An investigation of 2D multizone surround sound systems," in *Proc. 125th Audio Engineering Society Convention*, San Francisco, CA, Oct. 2008, pp. 1-9.

[10] T. Betlehem and C. Withers, "Sound field reproduction with energy constraint on loudspeaker weights," *IEEE Trans. Audio, Speech, and Language Process.*, vol. 20, no. 8, pp. 2388–2392, 2012.

[11] N. Radmanesh and I. S. Burnett, "Generation of isolated wideband sound field using a combined two-stage Lasso-LS algorithm," *IEEE Trans. Audio, Speech, and Language Process.*, vol. 21, no. 2, pp. 378–387, 2013.

[12] W. Jin and W. B. Kleijn, "Multizone soundfield reproduction in reverberant rooms using compressed sensing techniques," in *Proc. IEEE International Conference on Acoustics, Speech, and Signal Processing (ICASSP)*, Florence, Italy, May 2014, pp. 4728–4732.

[13] J.-H. Chang and F. Jacobsen, "Sound field control with a circular double-layer array of loudspeakers," *J. Acoust. Soc. Am.*, vol. 131, no. 6, pp. 4518–4525, 2012.

[14] J.-H. Chang and F. Jacobsen, "Experimental validation of sound field control with a circular double-layer array of loudspeakers," *J. Acoust. Soc. Am.*, vol. 133, no. 4, pp. 2046–2054, 2013.

[15] W. Jin, W. B. Kleijn, and D. Virette, "Multizone soundfield reproduction using orthogonal basis expansion," in *Proc. IEEE International Conference on Acoustics, Speech, and Signal Processing (ICASSP)*, Vancouver, Canada, May 2013, pp. 311–315.

[16] Y. Cai, M. Wu, and J. Yang, "Sound reproduction in personal audio systems using the least-squares approach with acoustic contrast control constraint," *J. Acoust. Soc. Am.*, vol. 135, no. 2, pp. 734–741, 2014.

[17] Y. Wu and T. D. Abhayapala, "Spatial multizone soundfield reproduction: Theory and design," *IEEE Trans. Audio, Speech, and Language Process.*, vol. 19, no. 6, pp. 1711–1720, 2011.

[18] W. Jin and W. B. Kleijn, "Theory and design of multizone soundfield reproduction using sparse methods," *IEEE/ACM Trans. Audio, Speech, and Language Process. Trans. Audio, Speech, and Language Process.*, vol. 23, no. 12, pp. 2343 – 2355, 2015.

[19] M. A. Poletti and F. M. Fazi, "An approach to generating two zones of silence with application to personal sound systems," *J. Acoust. Soc. Am.*, vol. 137, no. 2, pp. 598–605, 2015.

[20] W. Zhang, T. D. Abhayapala, T. Betlehem, and F. M. Fazi, "Analysis and control of multi-zone sound field reproduction using modal-domain approach," *J. Acoust. Soc. Am.*, vol. 140, no. 3, pp. 2134–2144, 2016.

[21] Y. Wu and T. D. Abhayapala, "Multizone 2D soundfield reproduction via spatial band stop filters," in *Proc. IEEE Workshop on Applications of Signal Processing to Audio and Acoustics (WASPAA)*, New Paltz, NY, Oct. 2009, pp. 309–312.

[22] J. Ahrens and S. Spors, "An analytical approach to sound field reproduction using circular and spherical loudspeaker distributions," *Acta Acustica united with Acustica*, vol. 94 , no. 6, pp. 988–999, 2008.

[23] W. Zhang and T. D. Abhayapala, "2.5D sound field reproduction in higher order Ambisonics," in *Proc. International Workshop on Acoustic Signal Enhancement (IWAENC)*, Juan Ies Pins, French Riviera, Sep. 2014, pp. 342–346.

[24] F. Winter, J. Ahrens, and S. Spors, "On analytic methods for 2.5-D local sound field synthesis using circular distributions of secondary sources," *IEEE/ACM Transactions on Audio, Speech, and Language Processing*, vol. 24, no. 5, pp. 914–926, 2016.

[25] T. Okamoto, "2.5D higher-order ambisonics for a sound field described by angular spectrum coefficients," in *Proc. IEEE International Conference on Acoustics, Speech, and Signal Processing (ICASSP)*, Shanghai, China, Mar. 2016, pp. 326–330.

[26] T. Okamoto, "Analytical approach to 2.5D sound field control using a circular double-layer array of fixed-directivity loudspeakers," in *Proc. IEEE International Conference on Acoustics, Speech, and Signal Processing (ICASSP)*, New Orleans, USA, Mar. 2017, pp. 91–95.

[27] R. A. Kennedy, P. Sadeghi, T. D. Abhayapala, and H. M. Jones, "Intrinsic limits of dimensionality and richness in random multipath fields," *IEEE Transa. Signal Process.*, vol. 55, no. 6, pp. 2542–2556, 2007.

[28] G. N. Watson, *A Treatise on the Theory of Bessel Functions*, Cambridge University Press, New York, 2nd edition, 1995.

[29] T. Betlehem and T. D. Abhayapala, "Theory and design of sound field reproduction in reverberant rooms," *J. Acoust. Soc. Am.*, vol. 117, no. 4, pp. 2100–2111, 2005.

[30] J. Allen and D. Berkley, "Image method for efficiently simulating small-room acoustics," *J. Acoust. Soc. Am.*, vol. 65, no. 4, pp. 943–950, 1979.